HHS Public Access

Author manuscript

Arch Biochem Biophys. Author manuscript; available in PMC 2021 August 26.

Published in final edited form as:

Arch Biochem Biophys. 2020 September 30; 691: 108482. doi:10.1016/j.abb.2020.108482.

Lipid composition modulates ATP hydrolysis and calcium phosphate mineral propagation by TNAP-harboring proteoliposomes

B.Z. Favarin[1,2], **M. Bolean**[1], **A.P. Ramos**[1], **A. Magrini**[3], **N. Rosato**[4], **J.L. Millán**[5], **M. Bottini**[4,5,*], **A.J. Costa-Filho**[2], **P. Ciancaglini**[1,*]

[1]Department of Chemistry, FFCLRP, University of São Paulo, Ribeirão Preto, SP, Brazil

[2]Department of Physics, FFCLRP, University of São Paulo, Ribeirão Preto, SP, Brazil

[3]Department of Biopathology and Imaging Diagnostics, University of Rome Tor Vergata, Rome, Italy

[4]Department of Experimental Medicine, University of Rome Tor Vergata, Rome, Italy

[5]Sanford Burnham Prebys Medical Discovery Institute, La Jolla, CA, USA.

Abstract

Bone biomineralization is mediated by a special class of extracellular vesicles, named matrix vesicles (MVs), released by osteogenic cells. The MV membrane is enriched in sphingomyelin (SM), cholesterol (Chol) and tissue non-specific alkaline phosphatase (TNAP) compared with the parent cells' plasma membrane. TNAP is an ATP phosphohydrolase bound to cell and MV membranes *via* a glycosylphosphatidylinositol (GPI) anchor. Previous studies have shown that the lipid microenvironment influences the catalytic activity of enzymes incorporated into lipid bilayers. However, there is a lack of information about how the lipid microenvironment controls the ability of MV membrane-bound enzymes to induce mineral precipitation. Herein, we used TNAP-harboring proteoliposomes made of either pure dimyristoylphosphatidylcholine (DMPC) or DMPC mixed with either Chol, SM or both of them as MV biomimetic systems to evaluate how the composition modulates the lipid microenvironment and, in turn, TNAP incorporation into the lipid bilayer by means of calorimetry. These results were correlated with the proteoliposomeś catalytic activity and ability to induce the precipitation of amorphous calcium phosphate (ACP) *in vitro*. DMPC:SM proteoliposomes displayed the highest efficiency of mineral propagation, apparent affinity for ATP and substrate hydrolysis efficiency, which correlated with their highest degree of membrane organization (highest ΔH), among the tested proteoliposomes. Results obtained from turbidimetry and Fourier transformed infrared (FTIR) spectroscopy showed that the tested proteoliposomes induced ACP precipitation with the order DMPC:SM>DMPC:Chol:SM≈DMPC:Chol>DMPC which correlated with the lipid organization and the presence of SM in the proteoliposome membrane. Our study arises important insights regarding the physical properties and role of lipid organization in MV-mediated mineralization.

*Corresponding authors: Pietro Ciancaglini : pietro@ffclrp.usp.br or Massimo Bottini : massimo.bottini@uniroma2.it.

Conflict of interest

All authors report no conflicts of interest.

Keywords

Matrix vesicle biomimetic systems; Biomineralization; Alkaline Phosphatase; Proteoliposome; Cholesterol; Sphingomyelin

1. Introduction

In vertebrates, bone biomineralization occurs through a highly regulated sequence of events leading to the ordered deposition of phosphate and calcium ions onto collagen fibers and the formation of calcium/phosphate mineral aggregates resembling the structure of hydroxyapatite (HA) ($Ca_{10}(PO_4)_6(OH)_2$). Osteoblasts are responsible for initiating this process through the release of a special class of extracellular vesicles, named matrix vesicles (MVs) [1–4]. The MV membrane is enriched in phospholipids, sphingomyelin (SM) and cholesterol (Chol) resembling the composition of lipid rafts found in the plasma membrane of parent cells [5, 6]. More specifically, the MV membrane consists of approximately 36% phosphatidylethanolamine (PE), 26.5% phosphatidylcholine (PC), 3.5% phosphatidic acid (PA), 7% phosphatidylinositol (PI) and 16.5% phosphatidylserine (PS) [7]. SM and Chol can compose up to 11% and 31.7%, respectively, of the total lipid mass of the MV membrane [8].

Lipid composition affects the organization of lipid bilayers. By comparing dimyristoylphosphatidylcholine (DMPC) and dipalmitoylphosphatidylcholine (DPPC) phase diagrams, Vist and Davis observed an increase in the ability to form thicker lipid bilayers with the length of the acyl chain [9, 10]. In terms of the effects of Chol on lipid bilayers, one of the main roles of Chol is to modulate the physical properties and lateral organization of lipid bilayers as well as the formation of lipid microdomains [11, 12]. For example, it has been shown that an increase in Chol concentration leads to a significant increase in the diffusion rate in DPPC:Chol mixtures [13]. Other studies have shown that adding Chol to DPPC liposomes decreases the phase transition enthalpy (ΔH) while increasing the vesicles' mean diameter [14–16]. ^{2}H NMR and calorimetric data have shown a suppression of the pre-transition in DPPC:Chol mixtures at Chol concentrations higher than approximately 6 mol% [9], and X-ray diffraction experiments have shown an increase in the repeat spacing of lipid bilayers made of DPPC and Chol as Chol concentration increases from 0 to 5% mol at temperatures in the gel phase region of the mixture [13, 17]. The presence of Chol also enables the formation of ordered lipid microdomains, named "lipid rafts", in biologic membranes [11]. The existence of heterogeneous microdomains in biologic membranes has been explained by the partition of lipid membranes in gel, liquid-disordered (L_d) and liquid-ordered (Lo) phases. Lipid rafts are microdomains in Lo phase enriched in Chol, SM, and uncharged glycolipids. They are characterized by distinct intermolecular interactions, including van der Waals interactions among the long and almost fully saturated chains of SM and glycosphingolipids, and hydrogen bonds between adjacent glycosyl portions of glycosphingolipids [6]. Furthermore, the long saturated acyl groups of sphingolipids can form more stable and compact associations with the planar and relatively rigid nucleus of Chol than with the shorter and generally unsaturated chains of phospholipids, which favors the formation of lipid rafts [18].

Lipid composition also affects the incorporation of proteins into lipid bilayers [16, 19]. The MV membrane contains a variety of hydrolytic enzymes, including tissue non-specific alkaline phosphatase (TNAP), a phosphomonohydrolase producing inorganic phosphate (P_i) from both pyrophosphate (PP_i) and adenosine-5-triphosphate (ATP). TNAP is incorporated into the outer leaflet of cell and MV membranes *via* a glycosylphosphatidylinositol (GPI) anchor, which promotes the lateral diffusion of the enzyme within the outer leaflet and accumulation in lipid microenvironments enriched in sphingolipids, glycosphingolipids and Chol [16, 17, 20, 21]. Previously, we have shown that the catalytic activity of TNAP is tailored by the local microenvironment [22, 23]. Different forms of TNAP (membrane associated, solubilized with detergent or treated with phosphatidylinositol-specific phospholipase C) showed different specificities for biologic substrates, indicating that the catalytic activity of the enzyme is greatly affected by both the presence of the GPI-anchor and the composition of the lipid membrane into which is inserted [15, 20]. Therefore, the effect of saturated and unsaturated lipids as well as of Chol on the MV-mediated biomineralization deserves special attention.

Recently, our group has developed proteoliposomes harboring TNAP made of a mixtures of DPPC, Chol and SM in different ratios as MV biomimetic systems to assess how the lipid composition affects the physical properties of the lipid membrane and TNAP incorporation and catalytic activity [16, 17, 24]. The use of liposomes with different lipid compositions can also help to assess how the lipid microenvironment affects the ability of enzymes incorporated into the MV membrane to induce mineral precipitation. Herein, we describe the fabrication of proteoliposomes with membranes in L_d phase composed by combinations of DMPC, Chol and SM [25–28] to understand how the lipid microenvironment modulates TNAP incorporation into the membrane and catalytic activity, and how these parameters correlate with the ability to promote the formation of amorphous calcium phosphate (ACP) *in vitro* in presence of a nucleator. This study sheds the light on the role of lipid composition in MV-mediated biomineralization.

2. Materials and Methods

2.1 Materials

All aqueous solutions were prepared using ultrapure apyrogenic water from a Millipore DirectQ system. Bovine serum albumin (BSA), trichloroacetic acid (TCA), tris hydroxymethyl-amino-methane (Tris), 2-amino-2-methyl-propan-1-ol (AMPOL), sodium dodecylsulfate (SDS), p-nitrophenyl phosphate disodium salt (pNPP), sodium adenosine-5-triphosphate (ATP), sodium dodecylsulphate (SDS), dexamethasone, β-glycerophosphate, polyoxyethylene-9-lauryl ether (polidocanol), dimysteroilphosphatidilcholine [DMPC, molecular weight (M_W)=677.93 g.mol^{-1}], cholesterol (Chol, M_W=386.65 g.mol^{-1}), sphyngomielin from bovine brain (SM, M_W=731.09 g.mol^{-1}, ≥ 97.0% pure), were purchased from Sigma Chemical Inc. (St Louis, MO). Sodium and magnesium chlorides were obtained from Merck KGaA (Darmstadt, Germany). Plastic culture flasks (75 cm^2) were obtained from Corning Inc. (Corning, NY). α-MEM, fetal bovine serum, ascorbic acid, gentamicin and fungizone were purchased from Gibco (Thermo Fisher Scientific Inc.,

Waltham, MA). All reagents were of analytical grade and used as received without further purification.

2.2. Preparation of alkaline phosphatase

Membrane-bound TNAP was extracted from rat bone marrow cells as described elsewhere [29]. TNAP (0.2 $mg.mL^{-1}$) was solubilized using 1 wt% polidocanol for 1 h under constant stirring, at 25°C. To remove the excess of detergent, 1 mL of polidocanol-solubilized enzyme was added to 200 mg of Calbiosorb resin as previously described [30] and the suspension was mixed for 2 h at 4°C. The detergent-free solubilized enzyme present in the supernatant was immediately used for incorporation into liposomes to avoid protein aggregation. The concentration of protein was estimated in the presence of 2 wt% SDS [31]. BSA was used as standard.

2.3. Measurements of TNAP enzymatic activity

p-Nitrophenylphosphatase (p-NPPase) activity was assayed discontinuously at 37°C by following the production of the yellowish product p-nitrophenolate ion (pNP^-) (ε=17,600 $M^{-1}.cm^{-1}$ at 1 M and pH 13) at 410 nm. Standard conditions were 50 mM Tris buffer, pH 7.4, containing 2 mM $MgCl_2$ and 10 mM pNPP in a final volume of 0.5 mL. The reaction was initiated by the addition of the enzyme and stopped with 0.5 mL of 1 M NaOH at appropriate time intervals [17]. ATPase activities were assayed discontinuously by measuring the amount of P_i produced in a final volume 0.5 mL according to a previously described procedure [32]. Standard assay conditions were 50 mM Tris buffer, pH 7.4, containing 2 mM $MgCl_2$ and substrate. The reaction was initiated by the addition of the enzyme and stopped with 0.25 mL of cold 30% trichloracetic acid at appropriate time intervals. All experiments were carried out in triplicate and the initial velocities were constant, provided that less than 5% of substrate was hydrolyzed. Controls in the absence of enzyme were included in each experiment to allow the nonenzymatic hydrolysis of the substrate. One enzyme unit (1 U) is defined as the amount of enzyme hydrolyzing 1.0 nmol of substrate per minute at 37 °C per milliliter or milligram of protein. Maximum velocity (V_{max}), apparent dissociation constant ($K_{0.5}$), and Hill coefficient (n_H) obtained from substrate hydrolysis were calculated as previously described [33]. Data were reported as the mean of triplicate measurements.

2.4. Preparation of liposomes and proteoliposomes

DMPC, Chol and SM were dissolved in chloroform in appropriate molar ratios and dried under a nitrogen flow. The resulting lipid film was kept under vacuum overnight and resuspended in 50 mM Tris-HCl buffer, pH 7.5, containing 2 mM $MgCl_2$. The mixture was incubated for 1 h at 60°C, above the critical phase transition temperature of the lipids, and vortexed at 10 min intervals. Large unilamellar liposomes (LUVs) were prepared by submitting the suspension to extrusion (eleven times) through 100 nm polycarbonate membranes in a LiposoFast extrusion system (Sigma-Aldrich). LUVs were prepared and used in the same day.

For proteoliposome preparation, equal volumes of liposomes (10 $mg.mL^{-1}$) and TNAP (0.02 $mg.mL^{-1}$) resulting in a 1:10,000 protein:lipid ratio in 50 mM Tris-HCl buffer, pH 7.5,

containing 2 mM $MgCl_2$, were mixed and incubated at 25°C for 1 h and ultracentrifuged at 100,000×*g* for 1 h. The pellet was resuspended in 50 mM Tris-HCl buffer, pH 7.5, containing 2 mM $MgCl_2$, to the original volume, obtaining proteoliposomes in a final lipid concentration of 10 mg.mL^{-1}. The activity of TNAP was measured in the supernatant and in the resuspended pellet (containing the proteoliposomes) in order to calculate the amount of protein incorporated into the proteoliposomes [31]. The size of liposomes and proteoliposomes were determined by dynamic light scattering (DLS) as described elsewhere [14] using a N5 Submicron Particle Size Analyser (Beckman Coulter Inc., Fullerton, CA). The value of the mean diameter was determined as the center of the size distribution peak. Average value (n=5) of the liposomes' diameter was obtained at 25 °C by unimodal distribution. The samples were filtered (0.8 μm) before the analysis.

2.5. Differential scanning calorimetry (DSC)

Phase transition temperature (T_c), enthalpy (ΔH) and cooperativity of phase transition ($\Delta t_{1/2}$) of the LUVs prepared with different lipid compositions were obtained by DSC. All LUV suspensions and reference buffers employed in the experiment were previously degasified under vacuum (140 mbar) for 15 min. The samples were scanned from 10 to 90 °C at an average heating rate of 0.5 °C.min^{-1} and the recorded thermograms were analyzed by using a Nano-DSC II - CSC (Waters, Milford, MA). A minimum of three heating and cooling scans were performed for each analysis and all thermograms were reproducible. In order to ensure the reproducibility of the results of the analysis of the effects of TNAP insertion and of the presence of microdomains on lipid phase transitions, we chose the simplest baseline correction to introduce the least amount of variability when comparing thermograms from different sets of experiments [14].

2.6. Mineralization assays with proteoliposomes and characterization by FTIR-spectroscopy

TNAP-containing proteoliposomes were incubated in SCL buffer in the presence of calcium phosphate-lipid complexes (PS-CPLX) at pH 7.5. SCL contained 2 mM Ca^{2+}, 104.5 mM Na^+, 133.5 mM Cl^-, 63.5 mM sucrose, 16.5 mM Tris, 12.7 mM K^+, 5.55 mM glucose, 1.83 mM HCO^{3-}, and 0.57 mM $MgSO_4$ [16, 17]. The assay was performed at saturating ATP concentrations (as source of P_i) for the measurement of the TNAP activity in each proteoliposome. Thus, ATP concentrations ranging from 10^{-6} to 10^{-2} M were used for the proteoliposomes composed of DMPC, DMPC:Chol, DMPC:SM and DMPC:Chol:SM, respectively. Enzyme-free liposomes were used as control. Mineral precipitation/propagation was measured by turbidity at 340 nm using a multi-well microplate assay as previously described [16]. Triplicate samples (280 μL) were poured into the wells of a 96-well microplate. Turbidity measurements were made after 10 s of agitation followed by 48 h of incubation at 37°C, by using a microplate reader (model SpectraMax® M3, Molecular Devices LLC, San Jose, CA). The results were normalized according to the protein concentration of each proteoliposome, since different amount of TNAP was incorporated depending on the lipid composition of the proteoliposome. The mineral samples were placed on the germanium crystal (4,000–600 cm^{-1}) of an attenuated total reflectance (ATR) accessory to assess the chemical groups by means of FTIR spectroscopy (model IRPrestige-21, Shimadzu Co., Tokyo, Japan). The efficacy of mineralization was assessed

by calculating the ratio between the areas of the band corresponding to the asymmetrical stretching of the PO_4^{3-} group at 1,032 cm^{-1} and the band of the carbonyl (C=O) group of the phospholipid at 1,680 cm^{-1}, used as internal reference [16, 17].

3. Results and discussion

3.1 Biophysical characterization of liposomes and proteoliposomes harboring TNAP.

We fabricated 4 different types of liposomes made of pure DMPC or mixed with 10% SM and/or 10% Chol (mol%). The diameter of the liposomes was evaluated by DLS. All the vesicles had an average diameter between 130 and 170 nm with a polydispersion index smaller than 0.2, suggesting the formation of monodisperse particles (Table 1) [15]. The diameter of DMPC liposomes was similar to that we have previously reported for DPPC liposomes [14]. The yield of TNAP incorporation into the membrane of DMPC liposomes through a GPI anchor was close to 65%, which was equivalent to 0.114 $\mu g.mL^{-1}$ of protein content. It is worth noting that this value is lower than the yield of TNAP incorporation into DPPC liposomes (~ 85%) [15, 17].

Although DMPC and DMPC:Chol liposomes had similar diameters, the yield of TNAP incorporation increased to almost 90% (0.156 $\mu g.mL^{-1}$ of protein) in the presence of Chol (Table 1). Interestingly, the yield of TNAP incorporation into DMPC:SM liposomes was close to 98%, whereas the yield of TNAP incorporation into DMPC:Chol:SM liposomes was approximately 77%. We posited that the incorporation of TNAP was favored by the lower fluidity and higher degree of organization of DMPC membranes in the presence of SM, Chol or both of them. Needham *et al.* and Snyder *et al.* studied the condensing effect of Chol in lipid membranes with several compositions [34, 35]. They showed that Chol is the single most influential factor in increasing bilayer cohesion. Moreover, Chol mixes more ideally in SM than in phosphatidylcholines of equal chain length [35]. The effect of Chol on the TNAP incorporation into DPPC monolayers was investigated by using Langmuir monolayers as membrane biomimetic systems [23]. Fluorescence and Brewster-angle micrographs revealed that the composition and Chol concentration in the monolayers influenced the formation and the dimension of TNAP-rich domains: higher Chol concentrations led to larger domains, indicating the preferential incorporation of the enzyme. According to Morandat (2002) [36], the insertion of TNAP into membranes is increased with addition of Chol in phosphatidylcholine liposomes. However, adding SM to DPPC-proteoliposomes caused a decrease in TNAP incorporation [37]. Hence, our data suggest that more compact lipid membranes are preferred for TNAP incorporation.

The DSC data revealed the presence of a single sharp peak centered at 23.8 °C and a ΔH=5.48 $kcal.mol^{-1}$ for DMPC liposomes, in agreement with the literature (Figure 1A and Table 2) [38]. We have previously found a ΔH=7.63 $kcal.mol^{-1}$ for DPPC liposomes. The difference in ΔH is due to the difference in the length of the carbonyl chains. The longer carbonyl chains of DPPC increased the van der Waals interactions within the lipid bilayer, which translated into a better lateral packing and a higher ΔH compared with DMPC [13]. The thermogram for DMPC:Chol liposomes (Figure 1B) displayed a main transition at 23.3 °C assigned to domains enriched in DMPC with ΔH=0.84 $kcal.mol^{-1}$, approximately 6 times lower than that for pure DMPC (5.48 $kcal.mol^{-1}$) (Table 2). The thermogram

for DMPC:Chol liposomes also displayed a transition at 25.3 °C related to lateral phase segregation and assigned to Chol-rich domains [39]. A similar curve profile assigned to lateral phase segregation was previously described for DPPC vesicles [14]. The thermogram for DMPC:SM liposomes displayed one peak at 24.6 °C (Figure 1C). Even though they had a slightly smaller ΔH, DMPC:SM liposomes displayed a cooperativity (expressed by the inverse of the full width at the half-maximum) $\Delta t_{1/2}$=2.03 °C, approximately double that of DMPC liposomes ($\Delta t_{1/2}$=0.98 °C) (Figure 1C and Table 2). This effect can be explained by the geometry of the SM molecule, which was not able to stabilize the lipid bilayer through hydrogen bonds and interactions between the hydrocarbon chains, leading to a less concerted transition (lower cooperativity) at higher temperatures [33, 34]. The thermogram obtained for DMPC:Chol:SM liposomes exhibited two peaks (Figure 1D) resembling the one obtained for DMPC:Chol liposomes (Figure 1B), suggesting that the amount of added SM (10 mol%) did not significantly affect the thermodynamic properties of DMPC:Chol liposomes. DMPC:Chol:SM liposomes displayed a main transition ΔH=1.11 kcal.mol^{-1}, which was approximately 5 times lower than that for liposomes made of pure DMPC (Table 2). Overall, the T_c of the main transition peak was not significantly different among the tested liposomes, however we found differences in ΔH values, which can be correlated with changes in the lipid organization due to the presence of Chol and/or SM within the DMPC bilayer.

The DSC thermograms obtained for the proteoliposomes harboring TNAP are shown in Figure 2, and the relative thermodynamic parameters are summarized in Table 2. The insertion of TNAP into DMPC liposomes through the GPI anchor resulted in the appearance of a second transition in the thermogram and an approximately 10-fold decrease in the ΔH value (from 5.48 to 0.65 kcal.mol^{-1}; Figure 2A and Table 2). In contrast, the insertion of TNAP into DMPC:Chol liposomes did not significatively change the value of phase transition ΔH, however a decrease of approximately 29% in the main transition cooperativity was observed ($\Delta t_{1/2}$ value from 1.58 to 1.12 °C; Table 2). Moreover, the peak assigned to Chol-rich domains (T_c = 25.3 °C) display a 3.4-fold decrease in the phase transition cooperativity ($\Delta t_{1/2}$ value from 0.49 to 1.67 °C; Table 2) in the presence of TNAP, showing an increase in the lateral phase segregation of Chol enriched domains. The peak associated to the phase transition observed for DMPC:SM proteoliposomes was broader compared with the corresponding liposomes (Figures 1C and 2C). Also, ΔH decreased of approximately 72% (from 5.07 to 1.40 kcal.mol^{-1}; Table 2). The thermograms for DMPC:Chol (Figure 2B) and DMPC:Chol:SM (Figure 2D) proteoliposomes were similar. Significant changes in the thermodynamic properties in the presence of TNAP were found for the ternary system with a decrease of 69% in the main phase transition ΔH (from 1.11 to 0.34 kcal.mol^{-1}; Table 2) and a decrease of 25% in the main transition $\Delta t_{1/2}$ (from 1.23 to 0.92 °C; Table 2). An increase in the lateral phase segregation of Chol-enriched domains in the ternary system (T_c = 25.1 °C, Figure 1D) due to the presence of TNAP (T_c = 25.4 °C, Figure 2D) was suggested by the 2.9-fold decrease in the phase transition cooperativity ($\Delta t_{1/2}$ value from 0.65 to 1.89 °C; Table 2). This phase segregation is even more pronounced in the presence of the enzyme, since the second peak became more resolved. A similar phenomenon was observed for proteoliposomes composed by DPPC:Chol:SM 80:10:10 (mol%) [3,15]. These results evidence the importance of both the organization and the composition of microdomains

in lipid bilayers during the reconstitution of TNAP. An overall decrease in the value of phase transition ΔH can be observed when comparing the thermodynamic parameters of the liposomes and proteoliposomes (Table 2). This result confirms that TNAP fluidized the lipid microenvironment, reducing the lipid-lipid interactions by inserting the GPI anchor [16].

3.2 Kinetic study of ATP hydrolysis by TNAP-proteoliposomes.

MVs bud from regions of the plasma membrane of osteogenic cells enriched in lipid rafts [3]. Since the MV membrane has a higher concentration of Chol, SM and longer chain fatty acids compared with the plasma membrane of parent cells [40–43], next we investigated the role of DMPC, Chol, and SM on the kinetic properties of TNAP incorporated into the membrane of MV-mimicking proteoliposomes.

ATP hydrolysis by TNAP-harboring proteoliposomes resulted in a sigmoidal saturation curve regardless of the lipid composition (Figure 3). The kinetic parameters were obtained by least-squares fitting of experimental data with Hill equation (Table 3). Addition of SM or a mixture of SM and Chol to DMPC proteoliposomes led to an approximately 9-fold increase in the apparent affinity for ATP, as suggested by a $K_{0.5}$ for ATP of 0.29±0.07 mM, 0.33±0.07 mM and 2.70±0.02 mM for DMPC:SM, DMPC:Chol:SM and DMPC, respectively, proteoliposomes (Table 3). Additionally, DMPC:SM and DMPC:Chol:SM proteoliposomes displayed a specificity constant ($k_{cat}/K_{0.5}$) of ATP hydrolysis one order of magnitude greater than that of DMPC and DMPC:Chol proteoliposomes. The positive effect of SM and Chol on the catalytic efficiency of ATP hydrolysis has been also described for TNAP-harboring DPPC proteoliposomes [16, 17]. However, the Hill coefficient n_H, which is a measure of the cooperativity between enzyme subunits, exhibited only slight differences among DMPC (n_H=1.3), DMPC:Chol (n_H=1.1) and DMPC:SM (n_H=1.4) proteoliposomes, but it was two-folds smaller for DMPC:Chol:SM proteoliposomes (n_H=0.6). These results suggest that, while the presence of SM in DMPC bilayers positively interfered with the orientation/positioning of the catalytic sites of TNAP as shown by the higher $k_{cat}/K_{0.5}$ value for DMPC:SM proteoliposomes compared with DMPC:proteoliposomes, the presence of Chol in DMPC bilayers had only a slight effect on the kinetic behavior of TNAP. However, when the sterol was added to DMPC:SM bilayers, it reduced by half the value of n_H, which translated into a less efficient mineral propagation of the ternary proteoliposomes compared with those made of DMPC:SM (see next section).

3.3 Propagation of biomineralization

After the release from osteogenic cells, MVs can initiate mineral precipitation by exploiting an intra-luminal nucleation core (NC) made of PS complexed to ACP and proteins (mostly Annexin A5) (PS complexes or PS-CPLXs) [44–46]. ACP is a kinetically unstable mineral formed when both Ca^{2+} and P_i are present in high concentrations (mM) [47–49]. PS-CPLXs are present at the early stages of development of almost all calcified tissues, including cartilage [50] and bone [45]. Although PS-CPLXs can induce the formation of HA *in vitro*, many factors have been posited to regulate their function *in vivo*, including pH, Ca^{2+}/P_i molar ratio and local lipid and protein microenvironments [8]. However, the precise role of such factors has not been thoroughly assessed as of yet.

In the last decade, several strategies to produce MV-mimicking proteoliposomes have been described [3, 15–17, 20, 24, 29, 51–56]. These proteoliposomes were made of DPPC, DOPC, SM, Chol, as well as lipids with different charges and loaded with proteins responsible for bone calcification [3, 15–17, 20, 24, 29, 51–56]. Nevertheless, these biomimetic models have been poorly exploited to evaluate specific aspects of MV-mediated biomineralization. Herein, we developed a biomineralization assay based on TNAP-harboring proteoliposomes as MV-mimicking systems to evaluate the maturation of PS-CPLXs *in vitro* by ATP hydrolysis in the presence of a nucleator. This approach differs from those described in the literature [46, 57] since the supersaturation condition of Ca^{2+} and P_i ions to initiate precipitation was not fulfilled. Instead, TNAP inserted in the proteoliposome membrane hydrolyzed the substrate (ATP) and produced P_i in the concentration required to mineralize, which very well mimics the sequence of events mediated by MVs during bone mineralization. As in previous studies [16, 17], the tests were carried out using the same amount of proteoliposomes harboring TNAP and at the V_{max} of ATP hydrolysis (substrate saturating condition) for each lipid composition of proteoliposomes.

Addition of Chol, SM or both of them to DMPC proteoliposomes promoted a 1.5, 2.6 and 1.5-fold increase, respectively, in the mineral propagation compared with pure DMPC (Figure 4). Interestingly DMPC:Chol and DMPC:Chol:SM proteoliposomes had similar efficiencies of mineral propagation, which correlated with the similarity of the lipid packing in the bilayers observed by means of DSC (Figures 2B and 2D). DMPC:SM proteoliposomes displayed the highest efficiency of mineral propagation, apparent affinity for ATP and substrate hydrolysis efficiency, which correlated with their highest degree of membrane organization (highest ΔH), among the tested proteoliposomes. Taken together, these results highlight the crucial role of the presence of Chol and SM, as well as of the lipid organization on the ability of mineral propagation by TNAP incorporated into a lipid bilayer (Table 3).

DMPC:Chol proteoliposomes exhibited an efficiency of mineral propagation approximately 65% higher than that of vesicles made of pure DMPC. A similar behavior was found for DPPC and DPPC:Chol proteoliposomes [16]. We posited that the presence of Chol increased the mechanical resistance and phase segregation of lipid bilayers [34], which, in turn, decreased the permeability of bilayers in L_d phase and led to a higher degree of disorder and a less lipid packing as suggested by the decrease in ΔH and cooperativity of phase transition (Table 2). Sabatini *et al.* described that the stability of lipid monolayers increases in the presence of Chol irrespective of the host matrix (either DMPC or DPPC) as indicated by the values of excess free energy of mixing calculated at values of surface pressure close to those found in natural membranes (30–35 $mN.m^{-1}$) [58]. Chol has several biological functions, among them the modulation of the physical properties and lateral organization of the plasma membrane lipid bilayer and, in turn, the activity of membrane proteins. Increased activity of TNAP upon insertion in biomimetic membranes containing Chol has been reported [16, 17, 20, 24, 56, 59–62]. A previous study has shown that the lipid microenvironment surrounding TNAP incorporated into bilayers is crucial for its catalytic activity [33]. Chol exerts both ordering and condensing effects on SM bilayers, due to the numerous H-bonds between Chol hydroxyl groups and SM polar groups [63]. Moreover, the phase segregation of Lo

(raft like) SM/Chol enriched domains in mixtures of low-melting temperature phospholipids [64] and the adsorption of TNAP in these domains may be responsible for the improved kinetics and mineralization properties of DMPC:SM:Chol proteoliposomes. Taken together, these results further validate that the catalytic sites of the GPI-anchored TNAP adopt different orientations depending on the composition and phase state of lipid membrane. Thus, the presence of Chol and/or SM, can interfere with the positioning of the catalytic sites of TNAP and, in turn, affects its kinetic behavior and efficiency to drive mineralization.

3.4 ATR-FTIR Spectroscopy

The differences in the efficiency of mineralization among the different types of proteoliposomes were further evaluated by means of ATR-FTIR spectroscopy (Figure 5). All ATR-FTIR spectra showed a broad band ranging from 3470 to 3410 cm^{-1} assigned to O-H stretching (not shown) [65]. Moreover, ATR-FTIR spectra for all proteoliposomes showed a band centered at approximately 1070 cm^{-1}, which is characteristic of apatite and related to the asymmetric stretching of the PO_4^{-3} group [16, 17, 66]. However, it was not possible to distinguish the phosphate signal arising from the mineral within the vesicles from that arising from the membrane. Thus, we calculated the changes in the ratio between the area under the curve (AUC) of the peaks assigned to PO_4^{3-} and C=O (~1730 cm^{-1}) before and after mineralization (Table 4). An increase in PO_4^{3-}/C=O ratio indicated the maturation of the nucleator in the presence of ATP, validating the hypothesis that the tested proteoliposomes were able to propagate mineralization.

In a previous study, Simão *et al.* described that the ratio between the relative intensities of the absorption bands assigned to the PO_4^{-3} and C=O groups was higher for TNAP-harboring DPPC proteoliposomes compared with DPPC proteoliposomes containing Chol and/or SM when the mineral precipitation was induced in absence of a nucleator [17]. This result showed that the addition of Chol and SM to proteoliposomes made of DPPC (in the gel phase at physiological temperatures) decreased the vesicle ability to form minerals. Conversely, herein we found that the addition of Chol and SM to proteoliposomes made of DMPC, which is in the L_d phase at physiological temperatures, led to an increase in the vesicle ability to propagate mineralization in the presence of a nucleator (Table 4). It is worth noting that the addition of SM led the a greater efficiency of mineral propagation compared with Chol for both DPPC [17] and DMPC proteoliposomes (Figure 4).

Although the two studies describe the ability of proteoliposomes harboring TNAP to induce (previous study by Simão *et al.* [17]) and propagate (current study) mineralization in the absence and in the presence, respectively, of a nucleator, they led to the main conclusion that TNAP-harboring bilayers made of phospholipids with lower transition temperatures have a higher biomineralization efficiency than bilayers made of phospholipids with higher transition temperatures.

4. Conclusions

Herein, we described how the presence of Chol and/or SM in the membrane of DMPC proteoliposomes harboring TNAP affects the enzyme incorporation and kinetic behavior, ATP hydrolysis and mineral propagation. The crucial role of the membrane organization

in the function of proteoliposomes could be highlighted by comparing the results obtained in this study for proteoliposomes made of DMPC (T_c = 23.8 °C) (Table 2) with those we have previously obtained for proteoliposomes made of DPPC (T_c = 41.5 °C) [14]. As the mineral propagation was carried out at 37 °C for both the systems, two scenarios were studied: mineralization by lipid membranes in the liquid phase (above the T_c for DMPC) and mineralization by lipid membranes in the gel phase (below the T_c for DPPC) [16]. These studies showed that DMPC proteoliposomes (in fluid phase) led to approximately 3-folds higher values of mineral propagation than DPPC proteoliposomes (in gel phase) [16].

We have previously found that an increase in the lipid complexity of the proteoliposome membrane led to a decrease in the activity of TNAP incorporated into DPPC-membranes through a GPI anchor [15]. In the present study, the yield of TNAP incorporation was higher for DMPC:SM liposomes than for neat DMPC, DMPC:Chol and DMPC:Chol:SM ones. DMPC:SM vesicles did not exhibit lateral phase segregation when compared with neat DMPC liposomes, suggesting that membranes containing SM formed distinct types of clusters than membranes containing Chol. The insertion of SM in the DMPC proteoliposomes stabilizes the membrane through hydrogen bonds between the hydrocarbon chains, which may explain the increase in the levels of mineral formation observed in DMPC:SM proteoliposomes compared with DMPC:Chol proteoliposomes.

The bilayers' lipid microenvironment also affects the kinetic behavior of the enzyme. We showed that DPMC-proteoliposomes containing Chol and SM were more efficient in inducing mineral propagation *in vitro* (with the order DMPC:SM>DMPC:Chol:SM~DMPC:Chol>DMPC).

In conclusion, we found that all tested proteoliposomes harboring TNAP propagate mineralization after 48 h of incubation in presence of ATP at saturating concentrations as a source of P_i and in presence of a nucleator. We also found that DMPC:SM proteoliposomes displayed the highest efficiency of mineral propagation, apparent affinity for ATP and substrate hydrolysis efficiency, which correlated with their highest degree of membrane organization (highest ΔH), among the tested proteoliposomesThis hypothesis will be also validated in our next investigations by using microscopic and spectroscopic approaches. Taken together, our results indicated that, in addition to the essential components required for mineralization, such as enzymes, substrates, ions and lipid bilayers, the degree of packing of lipid bilayers and the presence of sterol can affect both TNAP catalytic efficiency and the supersaturation conditions required to precipitate apatite crystals. Therefore, our study sheds the light on the crucial role of the lipid composition and, in turn, the physical properties and lipid organization of the bilayer on the apatite propagation driven by TNAP during MV-mediated mineralization.

Acknowledgements

We thank Fundação de Amparo à Pesquisa do Estado de São Paulo (FAPESP) (2014/00371-1, 2015/06814-5, 2016/21236-6, 2017/08892-9, 2018/12092-0), Coordenação de Aperfeiçoamento de Pessoal de Nível Superior - Brasil (CAPES) (Finance Code 001, #88887.320304/2019-00), and Conselho Nacional de Desenvolvimento Científico e Tecnológico (CNPq) (304021/2017-2) for the financial support given to our laboratory. BZF received FAPESP grant. MB received CAPES grant. PC and APR also acknowledges CNPq for research fellowships. This work was also supported in part by grant DE12889 from the National Institutes of Health (USA).

References

[1]. Golub EE, Role of matrix vesicles in biomineralization, Biochim Biophys Acta. 1790(12) (2009) 1592–8. doi: 10.1016/j.bbagen.2009.09.006.Epub 2009 Sep 26. [PubMed: 19786074]

[2]. Millan JL, The role of phosphatases in the initiation of skeletal mineralization, Calcif Tissue Int. 93(4) (2013) 299–306. doi: 10.1007/s00223-012-9672-8.Epub 2012 Nov 27. [PubMed: 23183786]

[3]. Bottini M, Mebarek S, Anderson KL, Strzelecka-Kiliszek A, Bozycki L, Simao AMS, Bolean M, Ciancaglini P, Pikula JB, Pikula S, Magne D, Volkmann N, Hanein D, Millan JL, Buchet R, Matrix vesicles from chondrocytes and osteoblasts: Their biogenesis, properties, functions and biomimetic models, Biochim Biophys Acta Gen Subj. 1862(3) (2018) 532–546. doi: 10.1016/j.bbagen.2017.11.005.Epub 2017 Nov 3. [PubMed: 29108957]

[4]. Yadav MC, Bottini M, Cory E, Bhattacharya K, Kuss P, Narisawa S, Sah RL, Beck L, Fadeel B, Farquharson C, Millan JL, Skeletal Mineralization Deficits and Impaired Biogenesis and Function of Chondrocyte-Derived Matrix Vesicles in Phospho1(−/−) and Phospho1/Pi t1 Double-Knockout Mice, J Bone Miner Res. 31(6) (2016) 1275–86. doi: 10.1002/jbmr.2790.Epub 2016 May 17. [PubMed: 26773408]

[5]. Lingwood D, Simons K, Lipid Rafts As a Membrane-Organizing Principle, Science327(5961) (2010) 46–50. [PubMed: 20044567]

[6]. Simons K, Coskun U, Grzybek M, Lingwood D, Levental I, Kaiser HJ, Lipid-protein interactions governing raft partitioning in membranes, Chem Phys Lipids163 (2010) S10–S10.

[7]. Thouverey C, Strzelecka-Kiliszek A, Balcerzak M, Buchet R, Pikula S, Matrix vesicles originate from apical membrane microvilli of mineralizing osteoblast-like Saos-2 cells, J Cell Biochem. 106(1) (2009) 127–38. doi: 10.1002/jcb.21992. [PubMed: 19009559]

[8]. Wuthier RE, Lipscomb GF, Matrix vesicles: structure, composition, formation and function in calcification, Front Biosci (Landmark Ed). 16 (2011) 2812–902. [PubMed: 21622210]

[9]. Vist MR, Davis JH, Phase equilibria of cholesterol/dipalmitoylphosphatidylcholine mixtures: 2H nuclear magnetic resonance and differential scanning calorimetry, Biochemistry. 29(2) (1990) 451–64. [PubMed: 2302384]

[10]. Boscia AL, Treece BW, Mohammadyani D, Klein-Seetharaman J, Braun AR, Wassenaar TA, Klosgen B, Tristram-Nagle S, X-ray structure, thermodynamics, elastic properties and MD simulations of cardiolipin/dimyristoylphosphatidylcholine mixed membranes, Chem Phys Lipids. 178 (2014) 1–10. doi: 10.1016/j.chemphyslip.2013.12.010. Epub 2013 Dec 28. [PubMed: 24378240]

[11]. Simons K, Ikonen E, Functional rafts in cell membranes, Nature. 387(6633) (1997) 569–72. [PubMed: 9177342]

[12]. Barenholz Y, Cholesterol and other membrane active sterols: from membrane evolution to “rafts”, Prog Lipid Res. 41(1) (2002) 1–5. [PubMed: 11694266]

[13]. Almeida PF, Carter FE, Kilgour KM, Raymonda MH, Tejada E, Heat Capacity of DPPC/Cholesterol Mixtures: Comparison of Single Bilayers with Multibilayers and Simulations, Langmuir. 34(33) (2018) 9798–9809. doi: 10.1021/acs.langmuir.8b01774.Epub 2018 Aug 8. [PubMed: 30088940]

[14]. Bolean M, Simao AM, Favarin BZ, Millan JL, Ciancaglini P, The effect of cholesterol on the reconstitution of alkaline phosphatase into liposomes, Biophys Chem. 152(1–3) (2010) 74–9. doi: 10.1016/j.bpc.2010.08.002.Epub 2010 Aug 14. [PubMed: 20810204]

[15]. Bolean M, Simao AM, Favarin BZ, Millan JL, Ciancaglini P, Thermodynamic properties and characterization of proteoliposomes rich in microdomains carrying alkaline phosphatase, Biophys Chem. 158(2–3) (2011) 111–8. doi: 10.1016/j.bpc.2011.05.019.Epub 2011 May 27. [PubMed: 21676530]

[16]. Favarin BZ, Andrade MAR, Bolean M, Simao AMS, Ramos AP, Hoylaerts MF, Millan JL, Ciancaglini P, Effect of the presence of cholesterol in the interfacial microenvironment on the modulation of the alkaline phosphatase activity during in vitro mineralization, Colloids Surf B Biointerfaces. 155 (2017) 466–476. doi: 10.1016/j.colsurfb.2017.04.051. Epub 2017 Apr 26. [PubMed: 28472750]

[17]. Simao AMS, Bolean M, Favarin BZ, Veschi EA, Tovani CB, Ramos AP, Bottini M, Buchet R, Millan JL, Ciancaglini P, Lipid microenvironment affects the ability of proteoliposomes harboring TNAP to induce mineralization without nucleators, J Bone Miner Metab15(10) (2018) 018–0962.

[18]. Edidin M, The state of lipid rafts: from model membranes to cells, Annu Rev Biophys Biomol Struct. 32:257–83.(doi) (2003) 10.1146/annurev.biophys.32.110601.142439.Epub 2003 Jan 16. [PubMed: 12543707]

[19]. Ciancaglini P, Yadav MC, Simao AM, Narisawa S, Pizauro JM, Farquharson C, Hoylaerts MF, Millan JL, Kinetic analysis of substrate utilization by native and TNAP-, NPP1-, or PHOSPHO1-deficient matrix vesicles, J Bone Miner Res. 25(4) (2010) 716–23. doi: 10.1359/jbmr.091023. [PubMed: 19874193]

[20]. Garcia AF, Simao AM, Bolean M, Hoylaerts MF, Millan JL, Ciancaglini P, Costa-Filho AJ, Effects of GPI-anchored TNAP on the dynamic structure of model membranes, Phys Chem Chem Phys. 17(39) (2015) 26295–301. doi: 10.1039/c5cp02377g. [PubMed: 26389140]

[21]. Ermonval M, Baychelier F, Fonta C, TNAP, an Essential Player in Membrane Lipid Rafts of Neuronal Cells, Subcell Biochem. 76:167–83.(doi) (2015) 10.1007/978-94-017-7197-9_9. [PubMed: 26219712]

[22]. Ciancaglini P, Simao AM, Camolezi FL, Millan JL, Pizauro JM, Contribution of matrix vesicles and alkaline phosphatase to ectopic bone formation, Braz J Med Biol Res. 39(5) (2006) 603–10. Epub 2006 Apr 20. [PubMed: 16648897]

[23]. Derradi R, Bolean M, Simao AMS, Caseli L, Millan JL, Bottini M, Ciancaglini P, Ramos AP, Cholesterol Regulates the Incorporation and Catalytic Activity of Tissue-Nonspecific Alkaline Phosphatase in DPPC Monolayers, Langmuir35(47) (2019) 15232–15241. [PubMed: 31702926]

[24]. Bolean M, Simao AMS, Barioni MB, Favarin BZ, Sebinelli HG, Veschi EA, Janku TAB, Bottini M, Hoylaerts MF, Itri R, Millan JL, Ciancaglini P, Biophysical aspects of biomineralization, Biophys Rev. 9(5) (2017) 747–760. doi: 10.1007/s12551-017-0315-1.Epub 2017 Aug 29. [PubMed: 28852989]

[25]. Bar LK, Barenholz Y, Thompson TE, Effect of sphingomyelin composition on the phase structure of phosphatidylcholine-sphingomyelin bilayers, Biochemistry. 36(9) (1997) 2507–16. doi: 10.1021/bi9625004. [PubMed: 9054556]

[26]. Trandum C, Westh P, Jorgensen K, Mouritsen OG, A thermodynamic study of the effects of cholesterol on the interaction between liposomes and ethanol, Biophys J. 78(5) (2000) 2486–92. doi: 10.1016/S0006-3495(00)76793-2. [PubMed: 10777745]

[27]. Mainali L, Raguz M, Subczynski WK, Formation of cholesterol bilayer domains precedes formation of cholesterol crystals in cholesterol/dimyristoylphosphatidylcholine membranes: EPR and DSC studies, J Phys Chem B. 117(30) (2013) 8994–9003. doi: 10.1021/jp402394m.Epub 2013 Jul 18. [PubMed: 23834375]

[28]. Goni FM, Alonso A, Bagatolli LA, Brown RE, Marsh D, Prieto M, Thewalt JL, Phase diagrams of lipid mixtures relevant to the study of membrane rafts, Biochim Biophys Acta. 1781(11–12) (2008) 665–84. doi: 10.1016/j.bbalip.2008.09.002.Epub 2008 Oct 7. [PubMed: 18952002]

[29]. Simao AM, Beloti MM, Cezarino RM, Rosa AL, Pizauro JM, Ciancaglini P, Membrane-bound alkaline phosphatase from ectopic mineralization and rat bone marrow cell culture, Comp Biochem Physiol A Mol Integr Physiol. 146(4) (2007) 679–87. Epub 2006 May 20. [PubMed: 16798036]

[30]. Camolezi FL, Daghastanli KR, Magalhaes PP, Pizauro JM, Ciancaglini P, Construction of an alkaline phosphatase-liposome system: a tool for biomineralization study, Int J Biochem Cell Biol. 34(9) (2002) 1091–101. [PubMed: 12009304]

[31]. Hartree EF, Determination of protein: a modification of the Lowry method that gives a linear photometric response, Anal Biochem. 48(2) (1972) 422–7. [PubMed: 4115981]

[32]. Kiffer-Moreira T, Sheen CR, Gasque KC, Bolean M, Ciancaglini P, van Elsas A, Hoylaerts MF, Millan JL, Catalytic signature of a heat-stable, chimeric human alkaline phosphatase with therapeutic potential, PLoS One. 9(2) (2014) e89374. doi: 10.1371/journal.pone.0089374.eCollection 2014. [PubMed: 24586729]

[33]. Simao AM, Yadav MC, Narisawa S, Bolean M, Pizauro JM, Hoylaerts MF, Ciancaglini P, Millan JL, Proteoliposomes harboring alkaline phosphatase and nucleotide pyrophosphatase as matrix vesicle biomimetics, J Biol Chem. 285(10) (2010) 7598–609. doi: 10.1074/jbc.M109.079830.Epub 2010 Jan 4. [PubMed: 20048161]

[34]. Needham D, Nunn RS, Elastic deformation and failure of lipid bilayer membranes containing cholesterol, Biophys J. 58(4) (1990) 997–1009. doi: 10.1016/S0006-3495(90)82444-9. [PubMed: 2249000]

[35]. Snyder B, Freire E, Compositional domain structure in phosphatidylcholine--cholesterol and sphingomyelin--cholesterol bilayers, Proc Natl Acad Sci U S A. 77(7) (1980) 4055–9. [PubMed: 6933455]

[36]. Morandat S, Bortolato M, Roux B, Cholesterol-dependent insertion of glycosylphosphatidylinositol-anchored enzyme, Biochim Biophys Acta. 1564(2) (2002) 473–78. [PubMed: 12175931]

[37]. Milhiet PE, Giocondi MC, Le Grimellec C, Cholesterol is not crucial for the existence of microdomains in kidney brush-border membrane models, J Biol Chem. 277(2) (2002) 875–8. Epub 2001 Nov 20. [PubMed: 11717303]

[38]. Bayerl TM, Werner GD, Sackmann E, Solubilization of DMPC and DPPC vesicles by detergents below their critical micellization concentration: high-sensitivity differential scanning calorimetry, Fourier transform infrared spectroscopy and freeze-fracture electron microscopy reveal two interaction sites of detergents in vesicles, Biochim Biophys Acta. 984(2) (1989) 214–24. [PubMed: 2765550]

[39]. Castillo N, Monticelli L, Barnoud J, Tieleman DP, Free energy of WALP23 dimer association in DMPC, DPPC, and DOPC bilayers, Chem Phys Lipids. 169 (2013) 95–105. doi: 10.1016/j.chemphyslip.2013.02.001. Epub 2013 Feb 13. [PubMed: 23415670]

[40]. Abdallah D, Hamade E, Abou Merhi R, Badran B, Buchet R, Mebarek S, Fatty acid composition in matrix vesicles and in microvilli from femurs of chicken embryos revealed selective recruitment of fatty acids, Biochem Bioph Res Co446(4) (2014) 1161–1164.

[41]. Balcerzak M, Hamade E, Zhang L, Pikula S, Azzar G, Radisson J, Bandorowicz-Pikula J, Buchet R, The roles of annexins and alkaline phosphatase in mineralization process, Acta Biochim Pol. 50(4):1019–38.(doi) (2003) 0350041019. [PubMed: 14739992]

[42]. Foster LJ, de Hoog CL, Mann M, Unbiased quantitative proteomics of lipid rafts reveals high specificity for signaling factors, P Natl Acad Sci USA100(10) (2003) 5813–5818.

[43]. Wuthier RE, Gore ST, Partition of inorganic ions and phospholipids in isolated cell, membrane and matrix vesicle fractions: evidence for Ca-Pi-acidic phospholipid complexes, Calcif Tissue Res. 24(2) (1977) 163–71. [PubMed: 597754]

[44]. Wu LN, Genge BR, Dunkelberger DG, LeGeros RZ, Concannon B, Wuthier RE, Physicochemical characterization of the nucleational core of matrix vesicles, J Biol Chem. 272(7) (1997) 4404–11. [PubMed: 9020163]

[45]. Boskey AL, Posner AS, Extraction of a calcium-phospholipid-phosphate complex from bone, Calcif Tissue Res. 19(4) (1976) 273–83. [PubMed: 3268]

[46]. Genge BR, Wu LN, Wuthier RE, In vitro modeling of matrix vesicle nucleation: synergistic stimulation of mineral formation by annexin A5 and phosphatidylserine, J Biol Chem. 282(36) (2007) 26035–45. Epub 2007 Jul 5. [PubMed: 17613532]

[47]. Eanes ED, Thermochemical studies on amorphous calcium phosphate, Calcif Tissue Res5(2) (1970) 133–45. [PubMed: 5423622]

[48]. Valhmu WB, Wu LN, Wuthier RE, Effects of Ca/Pi ratio, Ca2+ x Pi ion product, and pH of incubation fluid on accumulation of 45Ca2+ by matrix vesicles in vitro, Bone Miner. 8(3) (1990) 195–209. [PubMed: 2157511]

[49]. Von Euw S, Ajili W, Chan-Chang TH, Delices A, Laurent G, Babonneau F, Nassif N, Azais T, Amorphous surface layer versus transient amorphous precursor phase in bone - A case study investigated by solid-state NMR spectroscopy, Acta Biomater. 59 (2017) 351–360. doi: 10.1016/j.actbio.2017.06.040. Epub 2017 Jul 6. [PubMed: 28690009]

[50]. Wuthier RE, Lipids of mineralizing epiphyseal tissues in the bovine fetus, J Lipid Res. 9(1) (1968) 68–78. [PubMed: 5637432]

[51]. Simao AM, Beloti MM, Rosa AL, de Oliveira PT, Granjeiro JM, Pizauro JM, Ciancaglini P, Culture of osteogenic cells from human alveolar bone: a useful source of alkaline phosphatase, Cell Biol Int. 31(11) (2007) 1405–13. Epub 2007 Jun 28. [PubMed: 17689110]

[52]. Bolean M, Paulino Tde P, Thedei G Jr., Ciancaglini P, Photodynamic therapy with rose bengal induces GroEL expression in Streptococcus mutans, Photomed Laser Surg. 28 Suppl 1 (2010) S79–84. doi: 10.1089/pho.2009.2635.

[53]. Simao AM, Yadav MC, Ciancaglini P, Millan JL, Proteoliposomes as matrix vesicles' biomimetics to study the initiation of skeletal mineralization, Braz J Med Biol Res. 43(3) (2010) 234–41. [PubMed: 20401430]

[54]. Ciancaglini P, Simao AMS, Bolean M, Millan JL, Rigos CF, Yoneda JS, Colhone MC, Stabeli RG, Proteoliposomes in nanobiotechnology, Biophys Rev. 4(1) (2012) 67–81. doi: 10.1007/s12551-011-0065-4.Epub 2012 Jan 18. [PubMed: 28510001]

[55]. Bolean M, Simao AM, Kiffer-Moreira T, Hoylaerts MF, Millan JL, Itri R, Ciancaglini P, Proteoliposomes with the ability to transport Ca(2+) into the vesicles and hydrolyze phosphosubstrates on their surface, Arch Biochem Biophys. 584 (2015) 79–89. doi: 10.1016/j.abb.2015.08.018. Epub 2015 Aug 29. [PubMed: 26325078]

[56]. Bolean M, Izzi B, van Kerckhoven S, Bottini M, Ramos AP, Millan JL, Hoylaerts MF, Ciancaglini P, Matrix vesicle biomimetics harboring Annexin A5 and alkaline phosphatase bind to the native collagen matrix produced by mineralizing vascular smooth muscle cells, Biochim Biophys Acta Gen Subj. 1864(8) (2020) 129629. doi: 10.1016/j.bbagen.2020.129629. [PubMed: 32360152]

[57]. Wuthier RE, Rice GS, Wallace JE Jr., Weaver RL, LeGeros RZ, Eanes ED, In vitro precipitation of calcium phosphate under intracellular conditions: formation of brushite from an amorphous precursor in the absence of ATP, Calcif Tissue Int. 37(4) (1985) 401–10. [PubMed: 3930038]

[58]. Sabatini K, Mattila JP, Kinnunen PK, Interfacial behavior of cholesterol, ergosterol, and lanosterol in mixtures with DPPC and DMPC, Biophys J. 95(5) (2008) 2340–55. doi: 10.1529/biophysj.108.132076.Epub 2008 May 30. [PubMed: 18515391]

[59]. Derradi R, Bolean M, Simao AMS, Caseli L, Millan JL, Bottini M, Ciancaglini P, Ramos AP, Cholesterol Regulates the Incorporation and Catalytic Activity of Tissue-Nonspecific Alkaline Phosphatase in DPPC Monolayers, Langmuir. 35(47) (2019) 15232–15241. doi: 10.1021/acs.langmuir.9b02590.Epub 2019 Nov 14. [PubMed: 31702926]

[60]. Bolean M, Borin IA, Simao AMS, Bottini M, Bagatolli LA, Hoylaerts MF, Millan JL, Ciancaglini P, Topographic analysis by atomic force microscopy of proteoliposomes matrix vesicle mimetics harboring TNAP and AnxA5, Biochim Biophys Acta. 1859(10) (2017) 1911–1920. doi: 10.1016/j.bbamem.2017.05.010.Epub 2017 May 23.

[61]. Andrade MA, Favarin B, Derradi R, Bolean M, Simao AM, Millan JL, Ciancaglini P, Ramos AP, Pendant-drop method coupled to ultraviolet-visible spectroscopy: A useful tool to investigate interfacial phenomena, Colloids Surf A Physicochem Eng Asp. 504 (2016) 305–311. doi: 10.1016/j.colsurfa.2016.05.085. Epub 2016 May 27. [PubMed: 28190931]

[62]. Simao AM, Bolean M, Hoylaerts MF, Millan JL, Ciancaglini P, Effects of pH on the production of phosphate and pyrophosphate by matrix vesicles' biomimetics, Calcif Tissue Int. 93(3) (2013) 222–32. doi: 10.1007/s00223-013-9745-3.Epub 2013 May 31. [PubMed: 23942722]

[63]. Rog T, Pasenkiewicz-Gierula M, Cholesterol-sphingomyelin interactions: a molecular dynamics simulation study, Biophys J. 91(10) (2006) 3756–67. doi: 10.1529/biophysj.106.080887.Epub 2006 Aug 18. [PubMed: 16920840]

[64]. Garcia-Arribas AB, Alonso A, Goni FM, Cholesterol interactions with ceramide and sphingomyelin, Chem Phys Lipids. 199 (2016) 26–34. doi: 10.1016/j.chemphyslip.2016.04.002. Epub 2016 Apr 27. [PubMed: 27132117]

[65]. Ishikawa T, Wakamura M, Kondo S, Surface Characterization of Calcium Hydroxylapatite by Fourier-Transform Infrared-Spectroscopy, Langmuir5(1) (1989) 140–144.

[66]. Wuthier RE, Chin JE, Hale JE, Register TC, Hale LV, Ishikawa Y, Isolation and characterization of calcium-accumulating matrix vesicles from chondrocytes of chicken epiphyseal growth plate cartilage in primary culture, J Biol Chem. 260(29) (1985) 15972–9. [PubMed: 3905800]

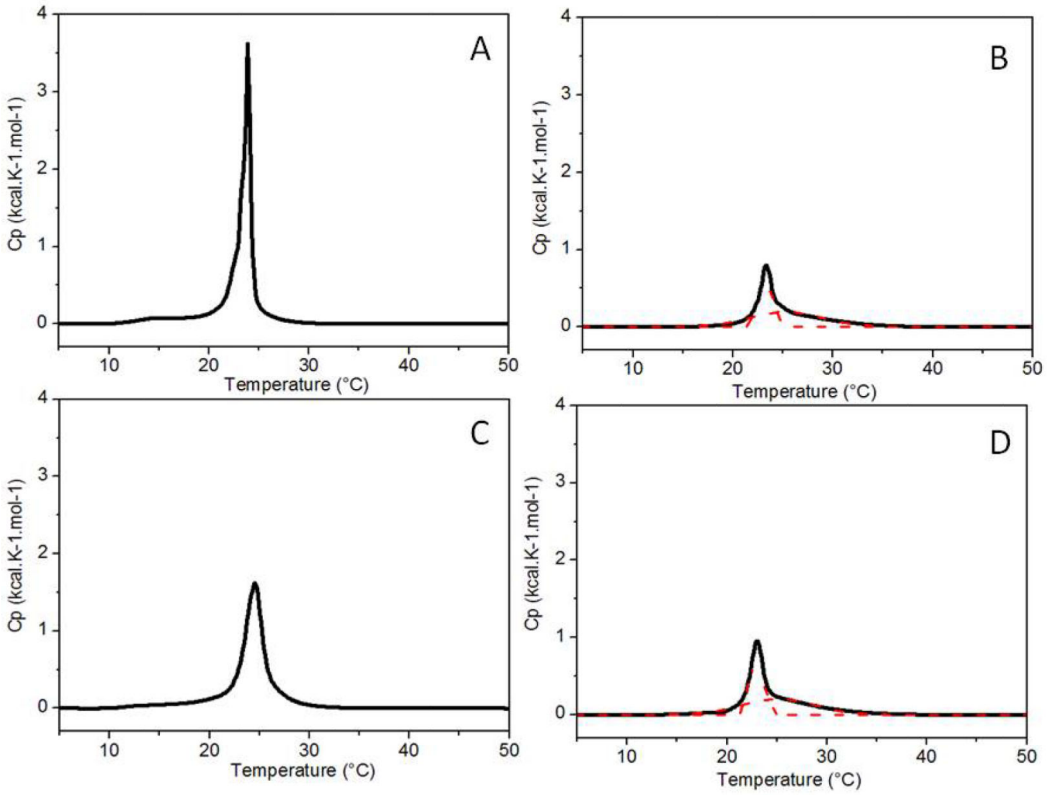

Figure 1:

DSC thermograms presented in excess heat capacity Cp (kcal.K^{-1}.mol^{-1}) as function of the Temperature (°C) for liposomes (10 mg/mL) composed of: **(A)** pure DMPC, **(B)** DMPC:Chol 90:10, **(C)** DMPC:SM 90:10 and **(D)** DMPC:Chol:SM 80:10:10, mol%. Dashed lines represent the best peak deconvolution.

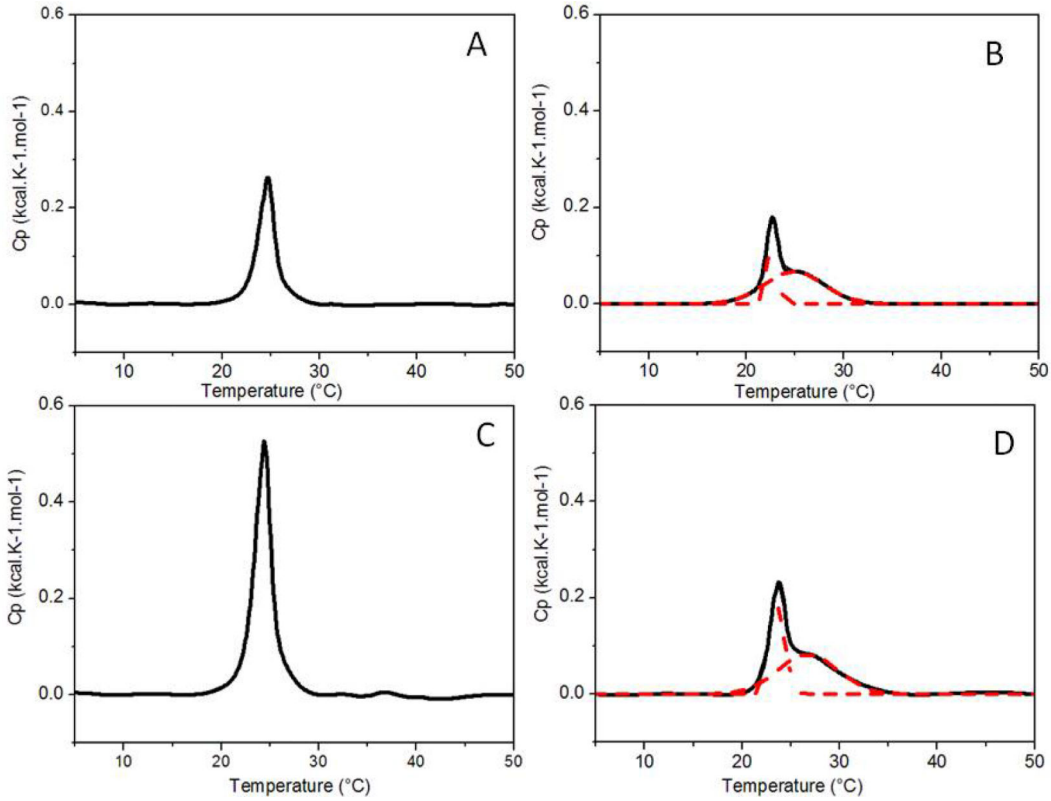

Figure 2:

DSC thermograms presented in excess heat capacity, Cp (kcal.K^{-1}.mol^{-1}) as function of the Temperature (°C) for proteoliposomes (10 mg/mL) composed of: **(A)** pure DMPC, **(B)** DMPC:Chol 90:10, **(C)** DMPC:SM 90:10 and **(D)** DMPC:Chol:SM 80:10:10, mol%. Dashed lines represent the best peak deconvolution.

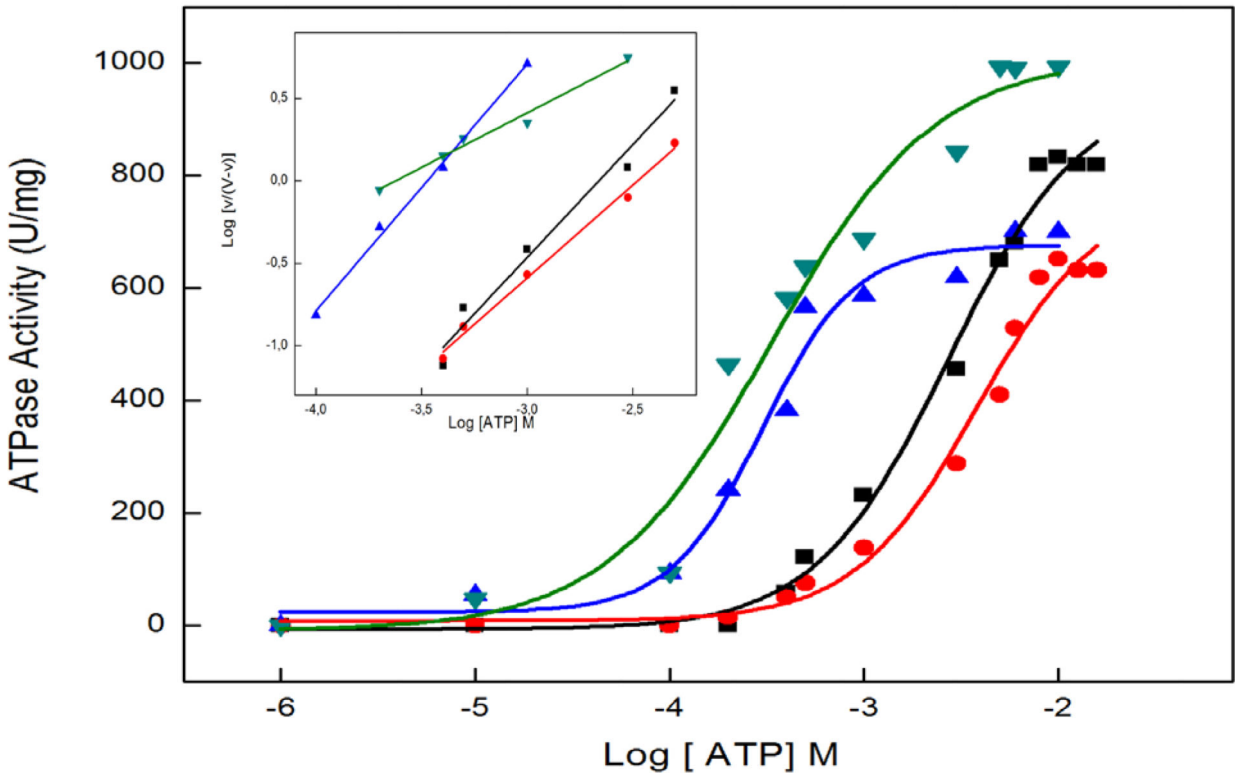

Figure 3:

Effect of ATP concentration on the enzymatic activity of reconstituted TNAP in liposomes composed of: (■) pure DMPC, (●) DMPC:Chol 90:10, (▲) DMPC:SM 90:10 and (▼) DMPC:Chol:SM 80:10:10, mol %. Inset: Hill coefficient (n_H).

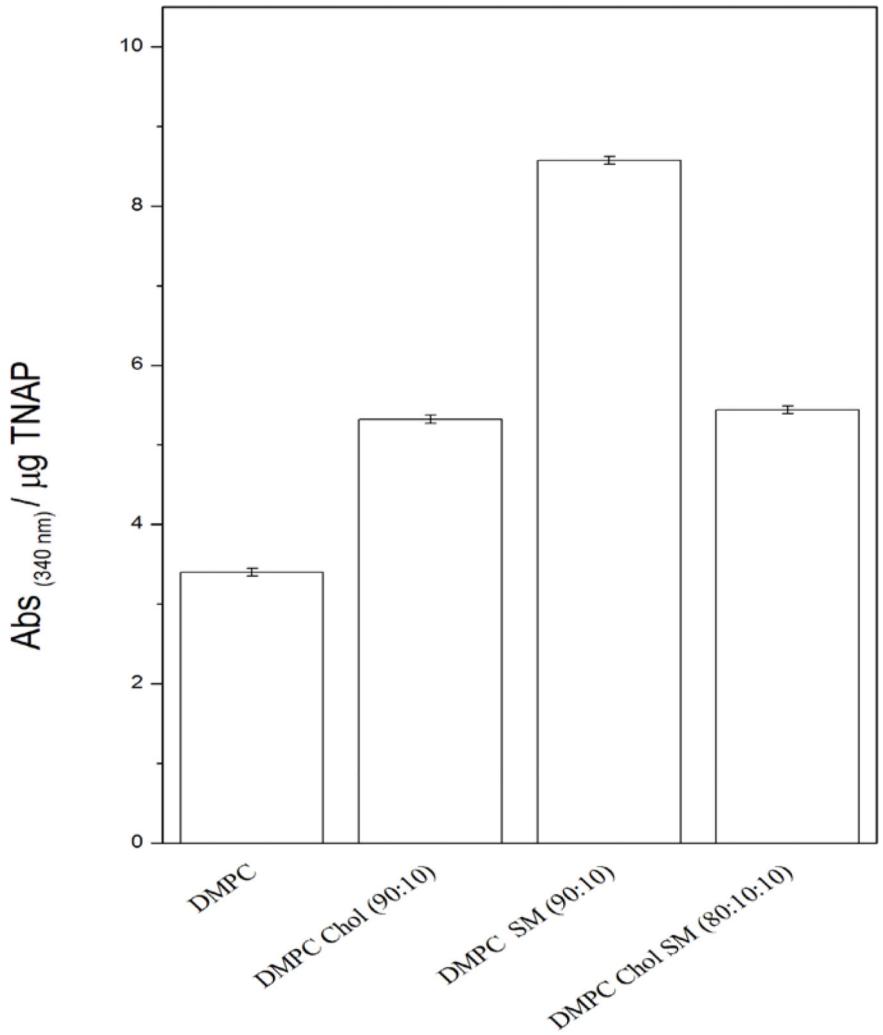

Figure 4:

Effect of lipid composition of TNAP-proteoliposomes (DMPC, DMPC:Chol 90:10, DMPC:SM 90:10 and DMPC:Chol:SM 80:10:10, mol %) on mineral propagation in the presence of a PS-CPLX nucleator at pH 7.5. The assay was accomplished using a saturating ATP concentration for each lipid composition as determined in the Figure 3 ranging from 10^{-6} to 10^{-2} M were used for proteoliposomes composed of DMPC, DMPC:Chol, DMPC:SM and DMPC:Chol:SM, respectively. Enzyme-devoid liposomes were used as control and bars show the increment in the absorbence after 48 h of incubation at 37 °C. All results are expressed as mean± SEM. $P<0.05$.

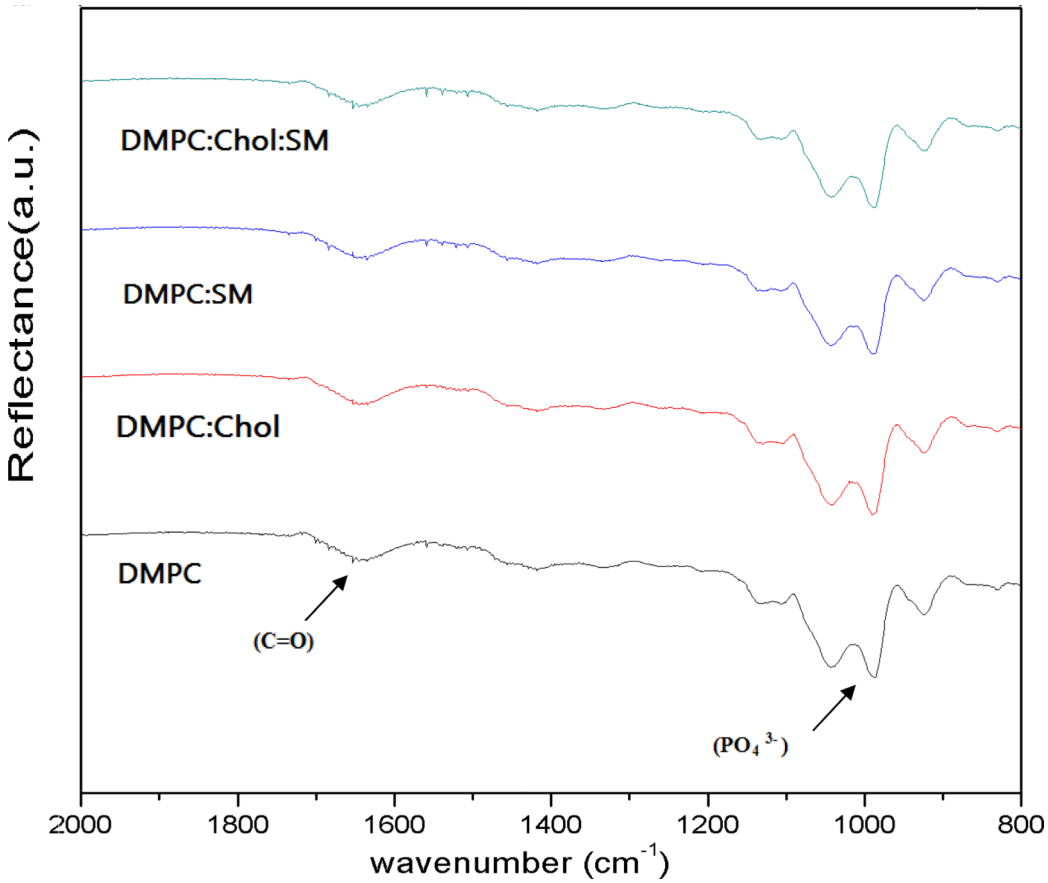

Figure 5:

FTIR spectra of the minerals obtained from the mineralization assays under incubation of TNAP-proteoliposomes composed of pure DMPC, DMPC:Chol 90:10, DMPC:SM 90:10 and DMPC:Chol:SM 80:10:10, mol %, in SCL buffer pH 7.5, at 37 °C, in the presence of a PS-CPLX nucleator. Mineralization was followed by the differences in the ratio between the areas of the internal reference band of the phospholipid (C=O) at 1730 cm^{-1} and the band corresponding to the asymmetrical stretching of the PO_4^{3-} group at 1070 cm^{-1}.

Table 1:

Effect of the lipid composition and the presence of protein on the average diameter of liposomes and proteoliposomes. Polydispersion values lower <0.2 for liposomes and proteoliposomes were obtained. Data are reported as the mean diameter ± S.D. of triplicate measurements of five different preparations.

		Liposome		Proteoliposome	
Lipid	**Composition (mol%)**	**Diameter (nm)**	**Diameter (nm)**	**Protein content (μg/mL)**	**Incorporation yield (%)**
DMPC	100	135.8±0.2	145.3±0.2	0.114±0.001	65.3
DMPC:Chol	90:10	139.5±0.3	167.5±0.3	0.156±0.003	89.5
DMPC:SM	90:10	134.2±0.4	138.6±0.1	0.172±0.002	98.6
DMPC:Chol:SM	80:10:10	145.2±0.5	150.6±0.7	0.134±0.004	76.8

Table 2:

Thermodynamic parameters of liposomes and proteoliposomes constituted by different lipids molar proportions.

Vesicles	(mol%)	Thermodynamic parameters			
		TNAP	ΔH (Kcal.mol^{-1})	T_C (°C)	$\Delta t_{1/2}$ (°C)
DMPC	100	−	5.48±0.31	23.8±0.2	0.98±0.12
		+	0.65±0.10 *	24.6±0.1	1.42±0.43
DMPC:Chol	90:10	−	0.84±0.12 *	23.3±0.3 *	1.58±0.23 *
			1.73±0.43	25.3±0.6	0.49±0.23
		+	0.86±0.10 *	23.3±0.4 *	1.12±0.61 *
			1.73±0.61	25.4±0.3	1.67±0.82
DMPC:SM	90:10	−	5.07±0.10	24.6±0.1	2.03±0.33
		+	1.40±0.11	24.4±0.2	1.82±0.41
DMPC:Chol:SM	80:10:10	−	1.11±0.23 *	22.9±0.4 *	1.23±0.22 *
			1.83±0.21	25.1±0.6	0.65±0.43
		+	0.34±0.10 *	2.9±0.1 *	0.92±0.42 *
			0.86±0.63	25.4 ±0.6	1.89±0.11

* Main transition

Table 3:

Kinetic parameters for ATP hydrolysis by TNAP reconstituted into DMPC-liposomes in different lipid compositions (mol%).

	Proteoliposomes (mol%)			
Kinect parameter	**DMPC**	**DMPC:Chol (90:10)**	**DMPC:SM (90:10)**	**DMPC:Chol:SM (80:10:10)**
V_{max} (U/mg)	833.2±13.4	652.3±11.2	701.3±13.2	993.8±12.5
$K_{0.5}$ (mM)	2.70±0.02	3.79±0.03	0.29±0.07	0.33±0.08
n_H	1.3±0.1	1.1±0.1	1.4±0.1	0.6±0.1
$k_{cat}/K_{0.5}$ ($M^{-1}.s^{-1}$)	6.2×10^2	3.4×10^2	4.7×10^3	6.0×10^3

Table 4:

Ratio between the relative intensities of the absorption bands in the infrared referring to the group. PO_4^{-3} (1070 cm^{-1}) and C=O (1730 cm^{-1}).

Proteolipossome	(mol%)	C=O (~1730 cm^{-1})	PO_4^{-3} (~1070 cm^{-1})	Ratio PO_4^{-3} / C=O
DMPC	100	684.72	1390.16	2.03 ± 0.12
DMPC:Chol	90:10	697.89	1461.28	2.09 ± 0.31
DMPC:SM	90:10	677.22	1491.88	2.20 ± 0.20
DMPC:Chol:SM	80:10:10	664.74	1507.32	2.27 ± 0.10